Collective multipartite Einstein-Podolsky-Rosen steering via cascaded four-wave mixing of rubidium atoms

Yang Liu,[1,2,3] Yin Cai,[1,*] Binshuo Luo,[1] Jin Yan,[1] Mengqi Niu,[1] Feng Li,[1] and Yanpeng Zhang[1]

[1]*Key Laboratory for Physical Electronics and Devices of the Ministry of Education and Shaanxi Key Lab of Information Photonic Technique, Xi'an Jiaotong University, Xi'an 710049, China*

[2]*State Key Laboratory of Transient Optics and Photonics, Xi'an Institute of Optics and Precision Mechanics, Chinese Academy of Sciences, Xi'an 710119, China*

[3]*University of Chinese Academy of Sciences, Beijing 100049, China*

(Received 26 May 2021; accepted 5 August 2021; published 7 September 2021)

Collective multipartite Einstein-Podolsky-Rosen (EPR) steering is a type of quantum correlation shared among n parties, where the EPR paradox of one party can be realized only by performing local measurements on all the remaining $n-1$ parties. Here, we propose an efficient method to produce collective multipartite EPR steering via symmetrically and asymmetrically cascading parametric amplification processes, i.e., four-wave mixing (FWM) of rubidium atoms. The simplified collective-steering criterion is introduced using the Coffman-Kundu-Wootters monogamy relation. Moreover, by actively adjusting the parametric gains, the collective EPR steerability is optimized in our schemes. We find that the scale of collective steering can be extended by cascading more FWMs; in particular, introducing optical loss is useful for generating collective steering with more parties only in the asymmetry structure. Our results pave the way for the construction of quantum networks and provide a promising candidate for one-sided device-independent quantum cryptography among multiple users.

DOI: 10.1103/PhysRevA.104.033704

I. INTRODUCTION

Einstein-Podolsky-Rosen (EPR) steering, which was first put forward to describe the "spooky action-at-a-distance" nonlocality phenomenon of Schrödinger [1], is an increasingly important concept in quantum mechanics. Suppose an EPR entangled state is shared between Alice and Bob, who are separated in remote space. If one observer, say, Alice, measures on her local particle A, the wave packet of Bob's particle B will collapse instantaneously. For the continuous-variable (CV) system, Alice and Bob share the quantum correlation in amplitude and phase quadratures, analogous to position and momentum for a particle. In 1989, Reid first demonstrated an experimental criterion via quadrature phase measurements [2]. Then, Wiseman formalized the concept of steering mathematically through violations of the local-hidden-state model [3] and, given a rigorous definition, revealed that a steerable state is a subset of the entangled state [4]. The inherent feature of EPR steering is a special type of quantum entanglement between Bell nonlocality [4] and EPR entanglement [5]. Due to the asymmetric property, EPR steering has been identified as a significant resource for quantum information processing, e.g., one-sided device-independent (1SDI) quantum key distribution [6–11], subchannel discrimination [12], and secure quantum teleportation [13,14].

In 2013, He and Reid developed the concept of genuine N-partite steering [15], which extended bipartite EPR steering to multipartite steering. Recently, multipartite steering was demonstrated experimentally using CV Gaussian states, i.e., multipartite EPR steering with optical networks [16], in four-mode cluster states [17], via a quantum frequency comb [18], and by separable states [19]. Collective multipartite steering, a special type of multipartite steering, was also presented [15,20–22], in which one party of the states can be steered only by the measurement of all the remaining $n-1$ parties, whereas it cannot be steered by a measurement on $n-2$ or fewer parties. This distinctive property of collective multipartite steering is relevant to the task of multimode quantum cryptography, such as quantum secret sharing (QSS) [23–28]. The conventional QSS process is that first, a dealer encodes a secret and distributes it into several parts and then sends the part information to the receivers; last, only all receivers working together can collaboratively decrypt the secret, and fewer receivers cannot get any information about the secret. Due to the intrinsic nature of collective steering, the security of this process is guaranteed, and we need not assume all the receivers are trustworthy. Therefore, it remarkably reduces the number of trustworthy devices in the quantum network and can provide an efficient implementation for 1SDI QSS [29].

Motivated by the demand for collective steering, a current challenge is to generate multimode entangled states. A promising candidate for producing quantum correlated twin beams (signal and idler) [30] and CV multipartite entanglement [31] is applying the single-pass parametric amplification process, i.e., the four-wave mixing (FWM) process in an atomic system. Using the FWM process to generate multipartite entanglement has several advantages, such as a strong third-order nonlinear effect, without the need for an optical cavity or extra beam splitter, spatially separated and well matched with the atomic transitions. Currently, due to its advantages, the single-pass FWM can be applied for quantum

*caiyin@xjtu.edu.cn

information [32–35] and quantum metrology [36], including entanglement imaging [37], four-wave slow light [38], delayed EPR entanglement [39], nonlinear interferometers [36,40,41], quantum noiseless amplification [42], a controllable graph state [31], a multiple-spatial-mode squeezed state [43], intensity-difference squeezing with dressed states [44], orbital angular momentum multipartite entanglement [45,46], phase estimation [47], etc.

Therefore, it is desirable to deeply study how collective multipartite steering can be created via cascading parametric amplification processes, i.e., FWM. In previous works, tripartite steering and the monogamy relations within quadripartite steering based on cascaded FWM were investigated [48–50]. In this paper, we simplify the collective-steering criterion with the Coffman-Kundu-Wootters (CKW) monogamy relation. And we theoretically produce collective tripartite, quadripartite, and pentapartite steering via symmetric and asymmetric structures of cascaded FWMs. Moreover, we investigate maximizing the collective multipartite steerability by adjusting the parametric gains of FWMs. Last, we study the effect of optical losses on collective multipartite steering. By introducing optical losses, we obtain collective quadripartite and pentapartite steering in the asymmetric scheme. Our results indicate that the cascaded FWM processes can provide a promising and scalable platform for collective multipartite steering that is useful for constructing the quantum networks for 1SDI-QSS.

This paper is organized as follows. In Sec. II, we present the criteria of bipartite EPR steering and collective multipartite steering. In Sec. III, we achieve collective multipartite steering via the symmetric and asymmetric cascaded FWM processes and analyze the collective regions with different gain parameters. In Sec. IV we study the effect of losses on the collective multipartite steering. Finally, we summarize in Sec. V.

II. THE PROPERTIES OF EPR STEERING AND MULTIPARTITE COLLECTIVE STEERING

Let us start by introducing the definition of bipartite EPR steering and explain the differences between bipartite EPR steering and multipartite collective steering in detail.

A. The steering criterion

A generic Gaussian state can be fully characterized by its covariance matrix (CM). We consider a Gaussian $(n_A + m_B)$-mode state of a bipartite system, composed of two subsystems: Alice (n modes) and Bob (m modes). We define the phase-space operators $\hat{X}^{A(B)}$ and $\hat{P}^{A(B)}$ for each mode and $\hat{\xi} = (\hat{X}_1^A, \hat{P}_1^A, \ldots, \hat{X}_n^A, \hat{P}_n^A, \hat{X}_1^B, \hat{P}_1^B, \ldots, \hat{X}_m^B, \hat{P}_m^B)^\top$, satisfying the canonical commutation relations $[\hat{\xi}_i, \hat{\xi}_j] = i\Omega_{ij}$, where $\Omega = \oplus_1^{n+m}\left(\begin{smallmatrix} 0 & 1 \\ -1 & 0 \end{smallmatrix}\right)$ is the symplectic form. The CM can be reconstructed in the form $\sigma_{AB} = \left(\begin{smallmatrix} \mathcal{A} & C \\ C^\top & \mathcal{B} \end{smallmatrix}\right)$ with elements $\sigma_{ij} = \langle \vec{\xi}_i \vec{\xi}_j + \vec{\xi}_j \vec{\xi}_i \rangle / 2 - \langle \vec{\xi}_i \rangle \langle \vec{\xi}_j \rangle$, where submatrices $\mathcal{A}$ and $\mathcal{B}$ correspond to Alice's and Bob's reduced states, respectively, and submatrix C stands for the correlation between them. The steerability from Alice to Bob ($A \to B$),

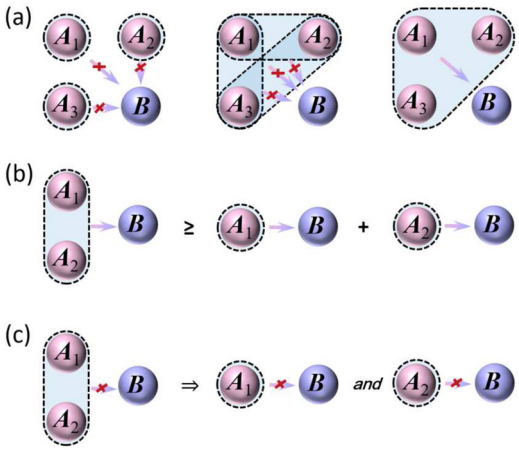

FIG. 1. (a) A simplified graph of collective multipartite steering, using collective quadripartite steering as an example. The possibilities among the steering party, i.e., A_1, A_2, A_3, (A_1, A_2), (A_1, A_3), (A_2, A_3), and (A_1, A_2, A_3) are depicted. (b) and (c) Simplified schematics of the CKW monogamy relation. Each circle denotes an optical mode, and arrows describe the bipartite steering between them; arrows with crosses represent nonsteerability.

corresponding to a $(n_A + m_B)$-mode Gaussian state, is quantified by [51]

$$\mathcal{G}^{A\to B}(\sigma_{AB}) = \max\left\{0, -\sum_{j:\bar{\nu}_j^{\mathcal{AB}/\mathcal{A}}<1} \ln\left(\bar{\nu}_j^{\mathcal{AB}/\mathcal{A}}\right)\right\}, \quad (1)$$

where $\bar{\nu}_j^{\mathcal{AB}/\mathcal{A}} (j = 1, \ldots, m_B)$ are the symplectic eigenvalues of $\bar{\sigma}_{\mathcal{AB}/\mathcal{A}} = \mathcal{B} - C^\top \mathcal{A}^{-1} C$, derived from the Schur complement of $\mathcal{A}$ in the CM σ_{AB}. The quantity $\mathcal{G}^{A\to B}$ is a monotonic function under Gaussian operations [52]. Bob can be steered by Alice iff $\mathcal{G}^{A\to B} > 0$ [51].

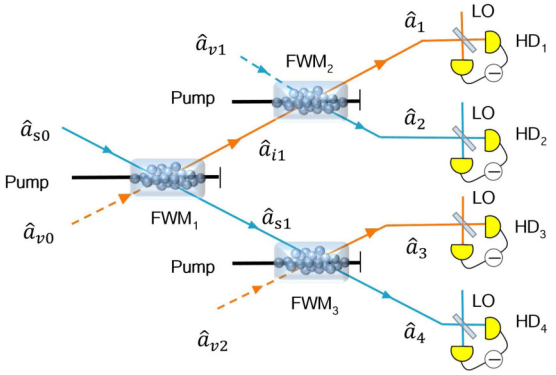

FIG. 2. Schematic diagram of the production of the four-mode entangled state via the symmetric-structure cascaded FWM system. $\hat{a}_{s_0}$ is seeded into FWM$_1$; $\hat{a}_{v_0}$, $\hat{a}_{v_1}$, and $\hat{a}_{v_2}$ are the three vacuum input modes; $\hat{a}_{i_1}$ and $\hat{a}_{s_1}$ are the output idler and signal beams of FWM$_1$; and $\hat{a}_{1,2,3,4}$ are the final four output modes after FWM$_2$ and FWM$_3$. LO denotes the local oscillator for homodyne detection (HD$_{1-4}$).

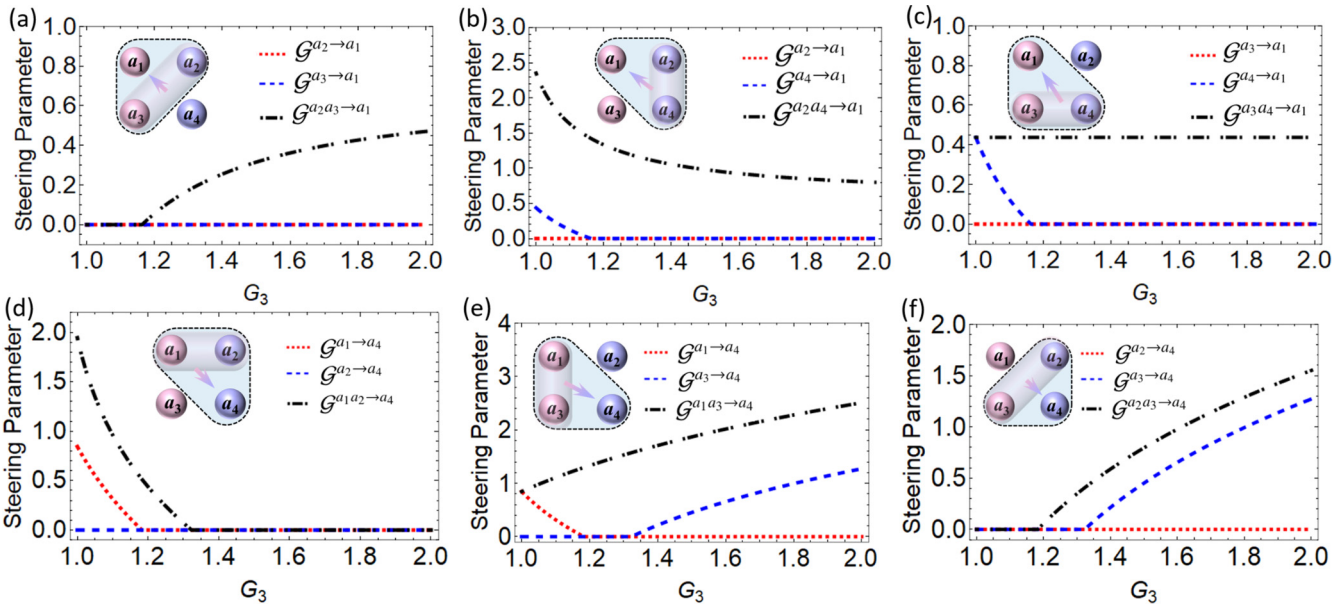

FIG. 3. Collective tripartite steering with a symmetric-structure cascaded FWM system. Variation of the (1+1)- and (2+1)-mode steering parameters with G_3 for $G_1 = 2$, $G_2 = 1.2$. $\hat{a}_1$ and $\hat{a}_3$ are the idler beams; $\hat{a}_2$ and $\hat{a}_4$ are the signal beams. (a)–(c) The steering from individual $\hat{a}_2$, $\hat{a}_3$, and $\hat{a}_4$ and any two of them to mode $\hat{a}_1$. (d)–(f) The steering from individual $\hat{a}_1$, $\hat{a}_2$, and $\hat{a}_3$ and any two of them to mode $\hat{a}_4$. The red dotted and blue dashed lines correspond to (1+1)-mode steering. The black dot-dashed lines correspond to (2+1)-mode steering.

B. The collective-steering criterion

We introduce a sufficient condition to quantify the multipartite collective steering. Without loss of generality, let us now formally define the collective quadripartite steering. The steered party B can be steered by only the modes (A_1, A_2, A_3) jointly, whereas a measurement on less than three modes cannot steer mode B, as indicated in Fig. 1(a); that is, (i) $\mathcal{G}^{A_1\to B} = \mathcal{G}^{A_2\to B} = \mathcal{G}^{A_3\to B} = \mathcal{G}^{A_1A_2\to B} = \mathcal{G}^{A_1A_3\to B} = \mathcal{G}^{A_2A_3\to B} = 0$, and (ii) $\mathcal{G}^{A_1A_2A_3\to B} > 0$. This requirement means that, for collective steering, the steering modes (A_1, A_2, A_3) in a remote location can collaboratively infer the higher-precision information such that the quantum standard limit corresponding to the bound of the EPR steering for the inferred amplitude and phase quadratures of steered mode B is violated [2,51], but when it has fewer than three modes, e.g., A_1, A_2, A_3, (A_1, A_2), (A_1, A_3), and (A_2, A_3), the information cannot be retrieved. The bound of the steering criteria [Eq. (2)] corresponds to the case when the two parties (Alice and Bob) are separable coherent states, relevant to the Heisenberg uncertainty.

Then we extend the collective-steering criterion to the n-partite case, which has one steered mode (B) and $n-1$ steering modes $(A_1, A_2, \ldots, A_{n-1})$. It is equivalent to the two simultaneous conditions

$$\begin{aligned} \mathcal{G}^{A'\to B} &= 0, \quad n_{A'} = 1, 2, \ldots, n-2, \\ \mathcal{G}^{A_1A_2\cdots A_{n-1}\to B} &> 0, \quad n_A = n-1, \end{aligned} \tag{2}$$

where A' is a subsystem of the steering party A with $n-2$ modes at most. If the two conditions are fulfilled at the same time, the multipartite collective steering is generated. Moreover, the multipartite steering from these Gaussian states follows the CKW monogamy inequality [52,53], which can help us understand the distributions of the quantum correlation in the systems. For a three-mode case, the CKW-type monogamy relation can be written as

$$\mathcal{G}^{A_1A_2\to B} \geqslant \mathcal{G}^{A_1\to B} + \mathcal{G}^{A_2\to B}, \tag{3}$$

where the steering party A consists of A_1 and A_2 in Fig. 1(b). This means that if (A_1, A_2) cannot steer B jointly, A_1 and A_2 cannot steer B individually, as shown in Fig. 1(c). Therefore, the above collective multipartite steering criterion can be simplified as

$$\begin{aligned} \mathcal{G}^{A'\to B} &= 0, \quad n_{A'} = n-2, \\ \mathcal{G}^{A_1A_2\cdots A_{n-1}\to B} &> 0, \quad n_A = n-1. \end{aligned} \tag{4}$$

We need to make sure only that A' with $n-2$ modes cannot steer mode B but A' with $n-1$ modes can. For instance, in the case of collective quadripartite and pentapartite steering, the simplified criteria require 4 and 5 constraints, while they contained 7 and 15 conditions in previous works [54], respectively. Note that the CKW monogamy relations may be shifted for $m_B > 1$ [50].

III. THE GENERATION OF MULTIMODE GAUSSIAN STATES AND COLLECTIVE MULTIPARTITE STEERING

Here, we construct collective multipartite steering via cascading single-pass parametric amplification process FWMs in symmetric and asymmetric structures. Note that the FWMs can also be taken as nonlinear beam splitters [49]. The nonlinear FWM interaction process is based on a double-Λ system between the hyperfine ground states $(5S_{1/2}, F = 2)$ and the excited states $(5P_{1/2})$ in Rb vapor at the $D1$ line [55]. The double-Λ scheme is a third-order nonlinear process that mixes an intense pump beam with a weak signal beam to generate an idler beam simultaneously. The pump beam was tuned ~0.8 GHz to the blue of the D_1 line, and the weak signal beam

was tuned ∼3.04 GHz to the red of the pump with an acousto-optic modulator. The amplified signal beam and the idler beam are cross coupled and have a strong quantum correlation. In addition, the phase-matching and energy-conservation conditions need to be satisfied in the FWM process. As shown in Fig. 2, $\hat{a}_{s_1} = G_1\hat{a}_{s_0} + g_1\hat{a}^\dagger_{v_0}$ and $\hat{a}_{i_1} = g_1\hat{a}^\dagger_{s_0} + G_1\hat{a}_{v_0}$ are the input-output relationship of the single FWM_1, where G_1 is the amplitude gain in the FWM_1 process and $G_1^2 - g_1^2 = 1$; $\hat{a}^\dagger_{s(v)_0}$ and $\hat{a}_{s(v)_0}$ stand for the creation and annihilation operators of the seed (vacuum) input; $\hat{a}_{s_1}$ and $\hat{a}_{i_1}$ stand for the annihilation operators of the output signal and idler beams, respectively. Similarly, we can apply the relationship of the single FWM process for the multiple cascaded FWM processes.

A. The symmetric cascaded FWM of four-mode entangled state

In this part, we first consider the case where three FWM processes are symmetrically cascaded. We take the signal and idler beams from the first FWM_1 process as the seed beams for FWM_2 and FWM_3, as illustrated in Fig. 2. The corresponding input-output relationship in these cascaded FWM processes can be written as [31]

$$\begin{bmatrix} \hat{X}_1^a \\ \hat{P}_1^a \\ \hat{X}_2^a \\ \hat{P}_2^a \\ \hat{X}_3^a \\ \hat{P}_3^a \\ \hat{X}_4^a \\ \hat{P}_4^a \end{bmatrix} = \begin{bmatrix} g_1G_2 & 0 & G_1G_2 & 0 & g_2 & 0 & 0 & 0 \\ 0 & -g_1G_2 & 0 & G_1G_2 & 0 & -g_2 & 0 & 0 \\ g_1g_2 & 0 & G_1g_2 & 0 & G_2 & 0 & 0 & 0 \\ 0 & g_1g_2 & 0 & -G_1g_2 & 0 & G_2 & 0 & 0 \\ G_1g_3 & 0 & g_1g_3 & 0 & 0 & 0 & G_3 & 0 \\ 0 & -G_1g_3 & 0 & g_1g_3 & 0 & 0 & 0 & G_3 \\ G_1G_3 & 0 & g_1G_3 & 0 & 0 & 0 & g_3 & 0 \\ 0 & G_1G_3 & 0 & -g_1G_3 & 0 & 0 & 0 & -g_3 \end{bmatrix} \begin{bmatrix} \hat{X}_{s_0} \\ \hat{P}_{s_0} \\ \hat{X}_{v_0} \\ \hat{P}_{v_0} \\ \hat{X}_{v_1} \\ \hat{P}_{v_1} \\ \hat{X}_{v_2} \\ \hat{P}_{v_2} \end{bmatrix}, \tag{5}$$

where $\hat{X}_{s(v)_i}$ and $\hat{P}_{s(v)_i}$ and $\hat{X}^a_{i+1}$ and $\hat{P}^a_{i+1} (i = 0, 1, 2, 3)$ are the amplitude and phase quadrature operators of the input and output signal and idler beams, which are defined as $\hat{X} = \hat{a} + \hat{a}^\dagger$ and $\hat{P} = i(\hat{a}^\dagger - \hat{a})$, respectively. G_i is the amplitude gain in the FWM_i process, and $G_i^2 - g_i^2 = 1$; $\hat{a}_i^\dagger$ and $\hat{a}_i$ stand for the creation and annihilation operators of the ith modes, respectively.

To demonstrate the collective tripartite steering of the symmetric cascaded FWM, we need to derive the CM, which can fully characterize the correlation properties of the produced four-mode Gaussian states. For Gaussian states, the elements of the CM are composed of covariances of amplitude and phase quadratures, which are defined as $\sigma_{ij} = \langle\vec{\xi}_i\vec{\xi}_j + \vec{\xi}_j\vec{\xi}_i\rangle/2 - \langle\vec{\xi}_i\rangle\langle\vec{\xi}_j\rangle$, where $\vec{\xi}_{\mathrm{sym4}} = (\hat{X}_1^a, \hat{P}_1^a, \hat{X}_2^a, \hat{P}_2^a, \hat{X}_3^a, \hat{P}_3^a, \hat{X}_4^a, \hat{P}_4^a)^\top$ and i and j denote the output optical modes. Because the cross correlations between the amplitude and phase quadratures do not exist, the corresponding covariances are all zero.

Then we are ready to quantify the collective tripartite steering shared among the four modes. In the symmetric cascaded system, mode $\hat{a}_1$ ($\hat{a}_4$) can steer $\hat{a}_2$ ($\hat{a}_3$) deterministically [50]. Therefore, $\hat{a}_2$ and $\hat{a}_3$ are not suitable for the steered modes to construct the collective tripartite steering. So six different partitions can achieve collective tripartite steering, i.e., $(\hat{a}_2, \hat{a}_3) \to \hat{a}_1$, $(\hat{a}_2, \hat{a}_4) \to \hat{a}_1$, $(\hat{a}_3, \hat{a}_4) \to \hat{a}_1$, $(\hat{a}_1, \hat{a}_2) \to \hat{a}_4$, $(\hat{a}_1, \hat{a}_3) \to \hat{a}_4$, and $(\hat{a}_2, \hat{a}_3) \to \hat{a}_4$. Based on these partitions, we get the analytical solution to (1+1)- and (2+1)-mode EPR steering of the symmetrical structure ($G_1 > 1, G_2 > 1$, and $G_3 > 1$):

$$\mathcal{G}^{a_1\to a_4} = \begin{cases} 0, & G_3 \geqslant \sqrt{\frac{2G_1^2G_2^2-1}{G_1^2(2G_2^2-1)}}, \\ -\ln\left(\frac{2G_1^2G_3^2(2G_2^2-1)}{2G_1^2G_2^2-1} - 1\right), & G_3 < \sqrt{\frac{2G_1^2G_2^2-1}{G_1^2(2G_2^2-1)}}, \end{cases} \tag{6a}$$

$$\mathcal{G}^{a_2\to a_4} = \begin{cases} 0, & G_3 \geqslant \sqrt{\frac{2G_1^2(G_2^2-1)+1}{G_1^2(2G_2^2-1)}}, \\ -\ln\left(\frac{2G_1^2G_3^2(2G_2^2-1)}{2G_1^2(G_2^2-1)+1} - 1\right), & G_3 < \sqrt{\frac{2G_1^2(G_2^2-1)+1}{G_1^2(2G_2^2-1)}}, \end{cases} \tag{6b}$$

$$\mathcal{G}^{a_3\to a_4} = \begin{cases} 0, & G_3 \leqslant \frac{\sqrt{2G_1^2-1}}{G_1}, \\ -\ln\left(\frac{2G_1^2-1}{2G_1^2G_3^2-2G_1^2+1}\right), & G_3 > \frac{\sqrt{2G_1^2-1}}{G_1}, \end{cases} \tag{6c}$$

$$\mathcal{G}^{a_1a_2\to a_4} = \begin{cases} 0, & G_3 \geqslant \frac{\sqrt{2G_1^2-1}}{G_1}, \\ -\ln\left(\frac{2G_1^2G_3^2}{2G_1^2-1} - 1\right), & G_3 < \frac{\sqrt{2G_1^2-1}}{G_1}, \end{cases} \tag{6d}$$

$$\mathcal{G}^{a_1a_3\to a_4} = -\ln\left(\frac{2G_1^2\left(G_2^2-1\right)+1}{2G_1^2(2G_2^2G_3^2-G_2^2-G_3^2+1)-1}\right), \quad G_3 > 1, \tag{6e}$$

$$\mathcal{G}^{a_2a_3\to a_4} = \begin{cases} 0, & G_3 \leqslant \sqrt{\frac{2G_1^2G_2^2-1}{G_1^2(2G_2^2-1)}}, \\ -\ln\left(\frac{2G_1^2G_2^2-1}{2G_1^2(2G_2^2G_3^2-G_2^2-G_3^2)+1}\right), & G_3 > \sqrt{\frac{2G_1^2G_2^2-1}{G_1^2(2G_2^2-1)}}. \end{cases} \tag{6f}$$

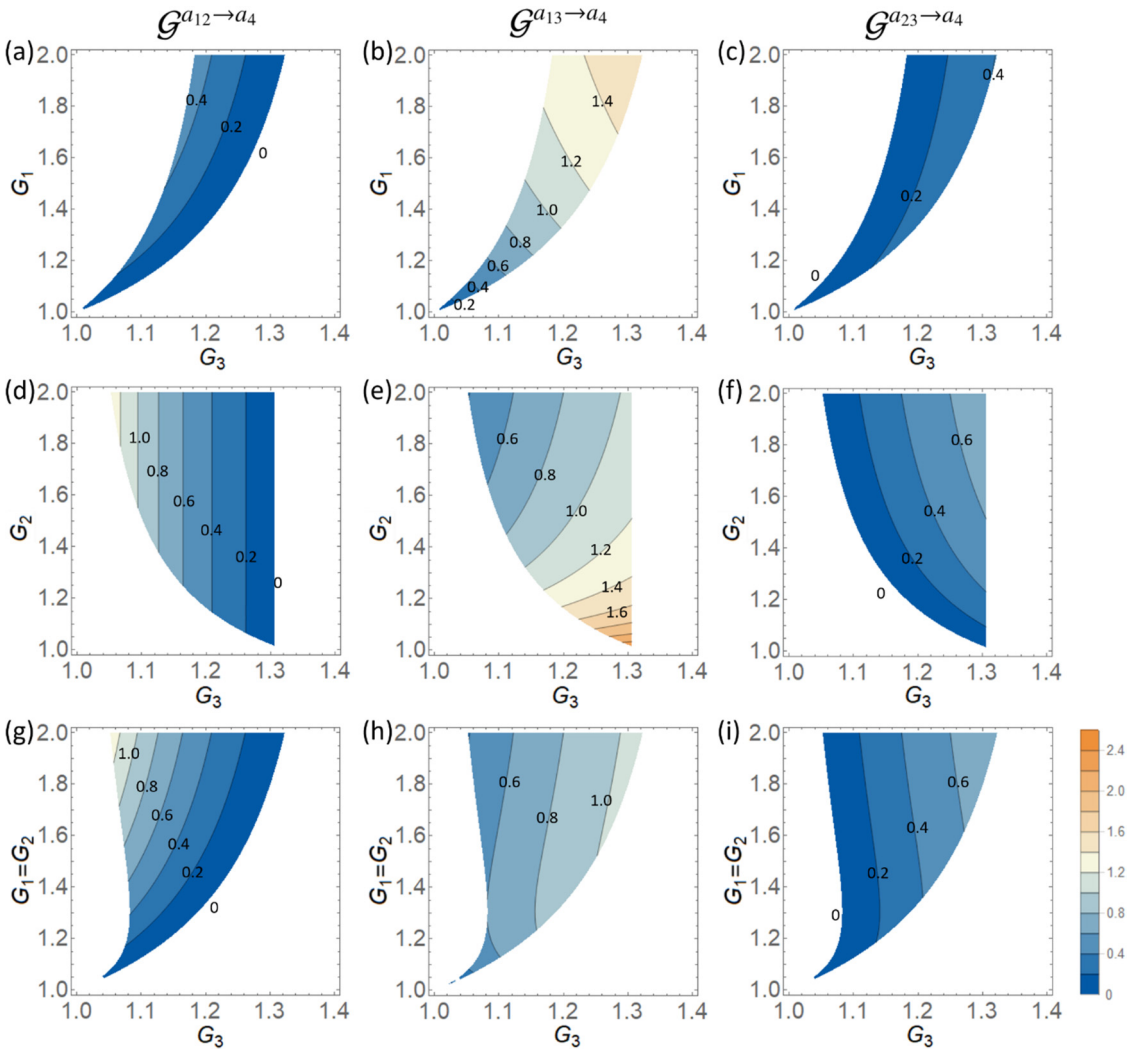

FIG. 4. Collective tripartite steering regions with the symmetric structure are examined by the steerability of (2+1) mode > 0 and (1+1) mode = 0. The steering parameters $\mathcal{G}^{a_1a_2\to a_4}$, $\mathcal{G}^{a_1a_3\to a_4}$, and $\mathcal{G}^{a_2a_3\to a_4}$ as a function of (a)–(c) G_1 and G_3 for $G_2 = 1.2$, (d)–(f) G_2 and G_3 for $G_1 = 2$, and (g)–(i) $G_1 = G_2$ and G_3, respectively. In the white areas, the criteria of collective multipartite steering are not satisfied, and thus, the collective tripartite steering does not exist.

As shown in Fig. 3, we quantify the (1+1)- and (2+1)-mode steering parameters with G_3 for $G_1 = 2$, $G_2 = 1.2$. Mode $\hat{a}_2$ cannot steer $\hat{a}_1$ due to the values of G_1 and G_2. Mode $\hat{a}_3$ also cannot steer $\hat{a}_1$ by itself because the modes of the same roles (signal and idler) cannot steer each other and they are not coupled to each other in the Hamiltonian. But its role in assisting joint steering with mode $\hat{a}_2$ is nontrivial when $G_3 > 1.16$. The range of gain parameter G_3 for $(\hat{a}_2, \hat{a}_3) \to \hat{a}_1$ is $G_3 \in (1.16, 2]$ in Fig. 3(a). Modes $(\hat{a}_2\hat{a}_4)$ can steer $\hat{a}_1$ deterministically, because all the signal (idler) beams that can steer all the idler (signal) ones or part of them. So we just need to make sure that $\hat{a}_2$ and $\hat{a}_4$ cannot steer $\hat{a}_1$ individually. When $G_3 \in [1.16, 2]$, we ensure $\mathcal{G}^{a_2\to a_1} = \mathcal{G}^{a_4\to a_1} = 0$ and $\mathcal{G}^{a_2a_4\to a_1} > 0$ simultaneously in Fig. 3(b). The maximum $\mathcal{G}^{a_2a_4\to a_1}$ is 1.42 at $G_3 \approx 1.16$. In Fig. 3(c), $\mathcal{G}^{a_3a_4\to a_1} \approx 0.44$, which is irrelevant to G_3. When $G_3 \in [1.16, 2]$, $\mathcal{G}^{a_3\to a_1}$ and $\mathcal{G}^{a_4\to a_1}$ both equal zero. The range of the gain parameter G_3 for $(\hat{a}_3, \hat{a}_4) \to \hat{a}_1$ is the same as that for $(\hat{a}_2, \hat{a}_4) \to \hat{a}_1$. In the symmetric structure, modes $\hat{a}_1$ and $\hat{a}_4$ and $\hat{a}_2$ and $\hat{a}_3$ play the same role in the system. So we can replace the modes with the others, i.e., $\mathcal{G}^{a_2\to a_1} = \mathcal{G}^{a_3\to a_4}$ and $\mathcal{G}^{a_1a_3\to a_4} = \mathcal{G}^{a_2a_4\to a_1}$. Accordingly, the associated gain parameters G_2 and G_3 also need to replace each other. When $G_3 < 1.32$, $\mathcal{G}^{a_1a_2\to a_4} > 0$, and $\mathcal{G}^{a_3\to a_4} = 0$ and vice versa. Similarly, when $G_3 > 1.18$, $\mathcal{G}^{a_2a_3\to a_4} > 0$, and $\mathcal{G}^{a_1\to a_4} = 0$; for $G_3 > 0.78$, $\mathcal{G}^{a_1a_3\to a_4} > 0$, and $\mathcal{G}^{a_2\to a_4} = 0$ in Figs. 3(d)–3(f). This result agrees with the CKW-type monogamy relation: $\mathcal{G}^{ij\to l} > 0 \Rightarrow \mathcal{G}^{k\to l} = 0$, which means two independent groups cannot steer the third single mode with Gaussian measurement simultaneously [50,56,57]. From the above analysis, The ranges of the gain parameter G_3 for $(\hat{a}_1, \hat{a}_2) \to \hat{a}_4$, $(\hat{a}_1, \hat{a}_3) \to \hat{a}_4$, and $(\hat{a}_2, \hat{a}_3) \to \hat{a}_4$ are $G_3 \in [1.18, 1.32)$, [1.18,1.32], and (1.18,1.32], respectively.

Now we investigate the collective tripartite steering as a function of G_1, G_2, and G_3 with the symmetric structure. As shown in Fig. 4, the contour-plot regions satisfy the collective-steering criterion, where $\hat{a}_i$ and $\hat{a}_j$ $(i, j = 1, 2, 3; i \neq j)$ cannot steer $\hat{a}_4$ individually but $\hat{a}_i\hat{a}_j$ jointly can steer $\hat{a}_4$. In order to study the effects of different gain parameters, the (1 + 2)-mode steering is varied with G_1 and G_3 for

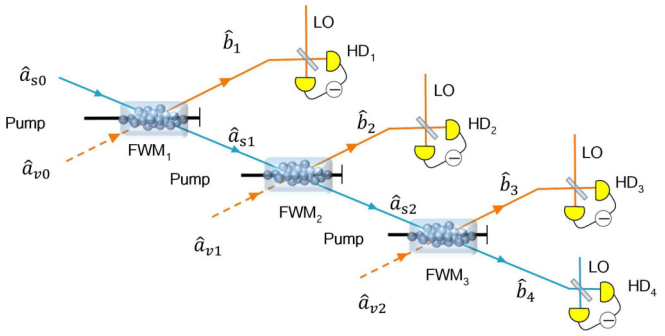

FIG. 5. Schematic diagram of producing the four-mode entangled state via an asymmetric structure. $\hat{a}_{s_0}$, $\hat{a}_{s_1}$, and $\hat{a}_{s_2}$ are seeded into FWM_1, FWM_2, and FWM_3, respectively. $\hat{a}_{v_0}$, $\hat{a}_{v_1}$, and $\hat{a}_{v_2}$ are the three vacuum input modes; $\hat{b}_{1,2,3,4}$ are the final four output modes. LO denotes the local oscillator for homodyne detection (HD_{1-4}).

$G_2 = 1.2$, G_2 and G_3 for $G_1 = 2$, or $G_1 = G_2$ and G_3 in Fig. 4. We can see $\mathcal{G}^{a_1a_2\to a_4}$ increases when adjusting G_1 from 1 to 2, is unchanged when adjusting G_2, and decreases when adjusting G_3 from 1 to 1.4, as shown in Figs. 4(a), 4(d) and 4(g). Note that the gain parameter G_2 does not affect the steerability $\mathcal{G}^{a_1a_2\to a_4}$. The reason is mainly that mode $\hat{a}_4$ participates in only the nonlinear processes FWM_1 and FWM_3 and is not coupled with FWM_2 in Eq. (6d). With the increase of gain parameter G_3, $\mathcal{G}^{a_1a_3\to a_4}$ significantly increases, and $\mathcal{G}^{a_2a_3\to a_4}$ remains the same. But with the increase of gain parameters G_1 and G_2, they show the opposite trend in Figs. 4(b), 4(c) 4(e), and 4(f). If we assume $G_1 = G_2$, $\mathcal{G}^{a_1a_3\to a_4}$ and $\mathcal{G}^{a_2a_3\to a_4}$ are nearly unchanged when adjusting $G_1 = G_2$. The reason is mainly that G_1 and G_2 have opposite effects on them and cause their destruction.

Furthermore, we find collective quadripartite steering cannot be obtained by the symmetric structure. According to the simplified criterion (4), we need to ensure that $\mathcal{G}^{lkp\to q} > 0$ and $\mathcal{G}^{lk\to q} = \mathcal{G}^{lp\to q} = \mathcal{G}^{kp\to q} = 0$ simultaneously, where k, l, p, and q represent the four modes. But the group of all the signal (idler) beams can steer all the idler (signal) ones or part of them deterministically, e.g., $\mathcal{G}^{a_2a_4\to a_1} > 0$ in Fig. 3(b) and $\mathcal{G}^{a_1a_3\to a_4} > 0$ in Fig. 3(e). According to the analytical solution with Eqs. 6(d)–6(f), G_1, G_2, and G_3 have no solution to satisfy these constraints at the same time, e.g., $\mathcal{G}^{a_1a_2\to a_4} = \mathcal{G}^{a_1a_3\to a_4} = \mathcal{G}^{a_2a_3\to a_4} = 0$. By introducing the optical loss, collective quadripartite steering also cannot be produced, as discussed in Sec. IV.

B. The asymmetric cascaded FWM of the four-mode entangled state

Now we move to investigate the case of three cascaded FWM processes with the asymmetric structure. The difference from the symmetric one is that we take the signal beams $\hat{a}_{s1}$ and $\hat{a}_{s2}$ as the seed beams for FWM_2 and FWM_3, respectively, as shown in Fig. 5. The corresponding input-output relationship in this structure can be written as

$$\begin{bmatrix} \hat{X}_1^b \\ \hat{P}_1^b \\ \hat{X}_2^b \\ \hat{P}_2^b \\ \hat{X}_3^b \\ \hat{P}_3^b \\ \hat{X}_4^b \\ \hat{P}_4^b \end{bmatrix} = \begin{bmatrix} g_1 & 0 & G_1 & 0 & 0 & 0 & 0 & 0 \\ 0 & -g_1 & 0 & G_1 & 0 & 0 & 0 & 0 \\ G_1g_2 & 0 & g_1g_2 & 0 & G_2 & 0 & 0 & 0 \\ 0 & -G_1g_2 & 0 & g_1g_2 & 0 & G_2 & 0 & 0 \\ G_1G_2g_3 & 0 & g_1G_2g_3 & 0 & g_2g_3 & 0 & G_3 & 0 \\ 0 & -G_1G_2g_3 & 0 & g_1G_2g_3 & 0 & g_2g_3 & 0 & G_3 \\ G_1G_2G_3 & 0 & g_1G_2G_3 & 0 & g_2G_3 & 0 & g_3 & 0 \\ 0 & G_1G_2G_3 & 0 & -g_1G_2G_3 & 0 & -g_2G_3 & 0 & -g_3 \end{bmatrix} \begin{bmatrix} \hat{X}_{s0} \\ \hat{P}_{s0} \\ \hat{X}_{v0} \\ \hat{P}_{v0} \\ \hat{X}_{v1} \\ \hat{P}_{v1} \\ \hat{X}_{v2} \\ \hat{P}_{v2} \end{bmatrix}. \tag{7}$$

Compared with the symmetrical structure, in the asymmetric cascaded system, modes $\hat{b}_4$ can steer $\hat{b}_1$, $\hat{b}_2$, and $\hat{b}_3$ deterministically [50]. Therefore, $\hat{b}_1$, $\hat{b}_2$, and $\hat{b}_3$ are not suitable for the steered modes to construct the collective tripartite steering. Only mode $\hat{b}_4$ can be steered by $\hat{b}_1$, $\hat{b}_2$, and $\hat{b}_3$ conditionally. So three different partitions can achieve collective tripartite steering, i.e., $(\hat{b}_1, \hat{b}_2) \to \hat{b}_4$, $(\hat{b}_1, \hat{b}_3) \to \hat{b}_4$, and $(\hat{b}_2, \hat{b}_3) \to \hat{b}_4$. The analytical solution to (1+1)- and (2+1)-mode EPR steering of the asymmetrical structure ($G_1 > 1$, $G_2 > 1$, and $G_3 > 1$) is

$$\mathcal{G}^{b_1\to b_4} = \begin{cases} 0, & G_3 \geqslant \frac{\sqrt{2G_1^2-1}}{G_1G_2}, \\ -\ln\left(\frac{2G_1^2G_2^2G_3^2}{2G_1^2-1} - 1\right), & G_3 < \frac{\sqrt{2G_1^2-1}}{G_1G_2}, \end{cases} \tag{8a}$$

$$\mathcal{G}^{b_2\to b_4} = \begin{cases} 0, & G_3 \geqslant \frac{\sqrt{2G_1^2(G_2^2-1)+1}}{G_1G_2}, \\ -\ln\left(\frac{2G_1^2G_2^2G_3^2}{2G_1^2(G_2^2-1)+1} - 1\right), & G_3 < \frac{\sqrt{2G_1^2(G_2^2-1)+1}}{G_1G_2}, \end{cases} \tag{8b}$$

$$\mathcal{G}^{b_3\to b_4} = \begin{cases} 0, & G_3 \leqslant \frac{\sqrt{2G_1^2G_2^2-1}}{G_1G_2}, \\ -\ln\left(\frac{2G_1^2G_2^2-1}{2G_1^2G_2^2G_3^2-2G_1^2G_2^2+1}\right), & G_3 > \frac{\sqrt{2G_1^2G_2^2-1}}{G_1G_2}, \end{cases} \tag{8c}$$

$$\mathcal{G}^{b_1b_2\to b_4} = \begin{cases} 0, & G_3 > \frac{\sqrt{2G_1^2G_2^2-1}}{G_1G_2}, \\ -\ln\left(\frac{2G_1^2G_2^2G_3^2}{2G_1^2G_2^2-1}-1\right), & G_3 \leqslant \frac{\sqrt{2G_1^2G_2^2-1}}{G_1G_2}, \end{cases} \tag{8d}$$

$$\mathcal{G}^{b_1b_3\to b_4} = \begin{cases} 0, & G_3 < \frac{\sqrt{2G_1^2(G_2^2-1)+1}}{G_1G_2}, \\ -\ln\left(\frac{2G_1^2G_2^2-2G_1^2+1}{2G_1^2G_2^2G_3^2-2G_1^2G_2^2+2G_1^2-1}\right), & G_3 \geqslant \frac{\sqrt{2G_1^2(G_2^2-1)+1}}{G_1G_2}, \end{cases} \tag{8e}$$

$$\mathcal{G}^{b_2b_3\to b_4} = \begin{cases} 0, & G_3 < \frac{\sqrt{2G_1^2-1}}{G_1G_2}, \\ -\ln\left(\frac{2G_1^2-1}{2G_1^2G_2^2G_3^2-2G_1^2+1}\right), & G_3 \geqslant \frac{\sqrt{2G_1^2-1}}{G_1G_2}. \end{cases} \tag{8f}$$

As shown in Fig. 6, we quantify the (1+1)- and (2+1)-mode steering parameters with G_3 for $G_1 = 2$, $G_2 = 1.2$. For the $(\hat{b}_1, \hat{b}_2) \to \hat{b}_4$ case, mode $\hat{b}_1$ cannot steer $\hat{b}_4$ when $G_3 \geqslant \frac{\sqrt{-1+2G_1^2}}{G_1G_2} \approx 1.10$, and $\hat{b}_2$ cannot steer $\hat{b}_4$ for the whole range. When $G_3 < \frac{\sqrt{2G_1^2G_2^2-1}}{G_1G_2} \approx 1.35$, modes $\hat{b}_1\hat{b}_2$ can steer $\hat{b}_4$ jointly. So for $G_3 \in [1.10, 1.35)$, we ensure $\mathcal{G}^{b_1\to b_4} = \mathcal{G}^{b_2\to b_4} = 0$ and $\mathcal{G}^{b_1b_2\to b_4} > 0$ simultaneously in Fig. 6(a). Similarly, for the $(\hat{b}_1, \hat{b}_3) \to \hat{b}_4$ case, the collective-steering range is $G_3 \in [1.10, 1.35]$ in Fig. 6(b). For the $(\hat{b}_2, \hat{b}_3) \to \hat{b}_4$ case, the collective-steering range is $G_3 \in (1.10, 1.35]$ in Fig. 6(c). From Fig. 6, it is seen that the (1+1)- and (2+1)-mode steering ranges are complementary; that is, when $G_3 < 1.10$, $\mathcal{G}^{b_1b_2\to b_4} > 0$, and $\mathcal{G}^{b_3\to b_4} = 0$, and when $G_3 > 1.10$, $\mathcal{G}^{b_1b_2\to b_4} = 0$, and $\mathcal{G}^{b_3\to b_4} > 0$. This result well agrees with a generalized from of the monogamy relation, which means two independent groups of modes cannot steer the third single mode with Gaussian measurements simultaneously ($\mathcal{G}^{kl\to q} > 0 \Rightarrow \mathcal{G}^{p\to q} = 0$ or $\mathcal{G}^{p\to q} > 0 \Rightarrow \mathcal{G}^{kl\to q} = 0$, where k, l, p, and q represent the four modes) [56]. With the increase of G_3, the function monotonicities of the (1+1)- and (2+1)-mode steerings are opposite; that is, $\mathcal{G}^{b_3\to b_4}$ increases with $G_3 > 1.35$ in Fig. 6(c), and $\mathcal{G}^{b_1b_2\to b_4}$ decreases with $G_3 < 1.35$ in Fig. 6(a). Due to the monogamy relation, the two conditions cannot be satisfied simultaneously. Figure 7 shows that using three asymmetric cascaded FWMs can create collective tripartite steering. The contoured regions satisfy the collective-steering criterion, in which $\hat{b}_i$ and $\hat{b}_j$ $(i, j = 1, 2, 3; i \neq j)$ cannot steer $\hat{b}_4$ individually but $\hat{b}_i\hat{b}_j$ jointly can steer $\hat{b}_4$. We investigate the steerability of the (2+1)-mode ($\mathcal{G}^{b_1b_2\to b_4}$, $\mathcal{G}^{b_1b_3\to b_4}$, and $\mathcal{G}^{b_2b_3\to b_4}$) as a function of G_1 and G_3 for $G_2 = 1.2$ in Figs. 7(a)–7(c), G_2 and G_3 for $G_1 = 2$ in Figs. 7(d)–7(f), and $G_1 = G_2$ and G_3 in Figs. 7(g)–7(i). We find that $\mathcal{G}^{b_1b_2\to b_4}$ increases with varying G_1 and G_2 from 1 to 2 and decreases with adjusting G_3 from 1 to 1.4, as shown in Figs. 7(a), 7(d) and 7(g). Compared with the symmetric FWM processes, the value of G_3 affects the steerability between modes $\hat{b}_1\hat{b}_2$ and $\hat{b}_4$ in the asymmetric FWM processes but does not affect the steerability between modes $\hat{a}_1\hat{a}_2$ and $\hat{a}_4$. Similarly, $\mathcal{G}^{b_1b_3\to b_4}$ increases with varying G_1 and G_3 from 1 to 2 and 1 to 1.4 but decreases with adjusting G_2 from 1 to 2 in Figs. 7(b), 7(e) and 7(h). $\mathcal{G}^{b_2b_3\to b_4}$ increases with varying G_2 and G_3 from 1 to 2 and 1 to 1.4 but decreases with adjusting G_1 from 1 to 2 in Figs. 7(c), 7(f) and 7(i). $\mathcal{G}^{b_1b_2\to b_4} \approx 1.421$ is maximized with experimentally feasible gain factors $G_1 \approx 1.336$, $G_2 = 1.2$, and $G_3 = 1$. $\mathcal{G}^{b_1b_3\to b_4} \approx 1.296$ is maximized with $G_1 = 2$, $G_2 = 1.2$, and $G_3 \approx 1.351$. $\mathcal{G}^{b_2b_3\to b_4} \approx 1.015$ is maximized with $G_1 = 1$, $G_2 = 1.2$, and $G_3 \approx 1.143$. Considering the specific FWM gain level of the experiment, this partition of $(\hat{b}_1, \hat{b}_2) \to \hat{b}_4$ is a good choice. If the gain of FWM_1 is greater than 2, then the partition of $(\hat{b}_1, \hat{b}_3) \to \hat{b}_4$ is a better one with a larger steerability. Note that, in Fig. 7, the three partitions of collective tripartite steering have very different gain dependence, but it is interesting to find that the area of the collective tripartite steering region is the same. This outcome is well explained by the monogamy relation of multipartite steering [50]. For instance, the upper left white area represents $\mathcal{G}^{b_1\to b_4} > 0$ in Figs. 7(a) and 7(b), and it also signifies $\mathcal{G}^{b_2b_3\to b_4} = 0$ in Fig. 7(c). Similarly, the lower left white area represents $\mathcal{G}^{b_2\to b_4} > 0$ and $\mathcal{G}^{b_1b_3\to b_4} = 0$, and the right white area denotes $\mathcal{G}^{b_3\to b_4} > 0$ and $\mathcal{G}^{b_1b_2\to b_4} = 0$. This pattern also fits the previous symmetric structures seen in Fig. 4.

Similar to the symmetric structure, the four-mode pure state produced by the asymmetric one still does not have collective quadripartite steering. For the $(\hat{b}_1, \hat{b}_2, \hat{b}_3) \to \hat{b}_4$ case, we cannot let the steerabilities $\mathcal{G}^{b_1b_2\to b_4}$, $\mathcal{G}^{b_1b_3\to b_4}$, and $\mathcal{G}^{b_2b_3\to b_4}$ be zero by adjusting G_3 simultaneously, as seen in Fig. 6. Moreover, we calculate the analytical solution with Eqs. 8(d)–8(f). The steerabilities $\mathcal{G}^{b_1b_2\to b_4}$, $\mathcal{G}^{b_1b_3\to b_4}$, and $\mathcal{G}^{b_2b_3\to b_4}$ equal zero when $G_1 = G_2 = G_3 = 1$. Obviously, these gains will induce no steering at all. Although there is no collective quadripartite EPR steering in pure states for either structure, we can obtain collective quadripartite steering in the asymmetric structure by introducing optical loss, which is given in more detail in Sec. IV.

C. The asymmetric cascaded FWM of the five-mode entangled state

We have studied the collective tripartite steering exhibited by the states generated by the symmetric and asymmetric schemes. It is interesting to study whether the above

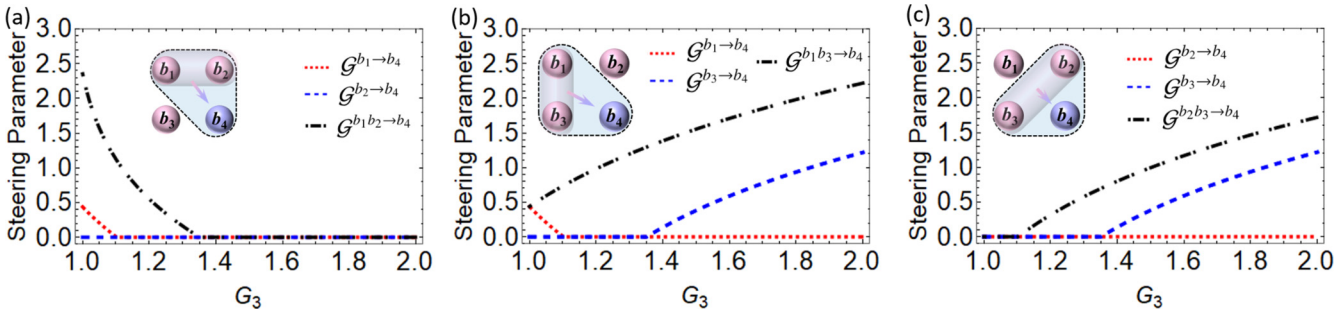

FIG. 6. Collective tripartite steering with the asymmetric structure of three cascaded FWMs. Variation of the (1+1)- and (2+1)-mode steering parameters with G_3 for $G_1 = 2$, $G_2 = 1.2$. $\hat{b}_1$, $\hat{b}_2$, and $\hat{b}_3$ are the idler beams; $\hat{b}_4$ is the signal beam. (a)–(c) The steering from individual $\hat{b}_1$, $\hat{b}_2$, and $\hat{b}_3$ and any two of them to mode $\hat{b}_4$. The red dotted and blue dashed lines correspond to (1+1)-mode steering.

schemes can scale to more parties and create collective multipartite EPR steering. So we investigate collective quadripartite steering in a five-mode entangled state in this section, first by generating the five-mode state and reconstructing its CM. Considering the case where four FWM processes are asymmetrically cascaded, we take the signal beam $\hat{a}_{s_i}$

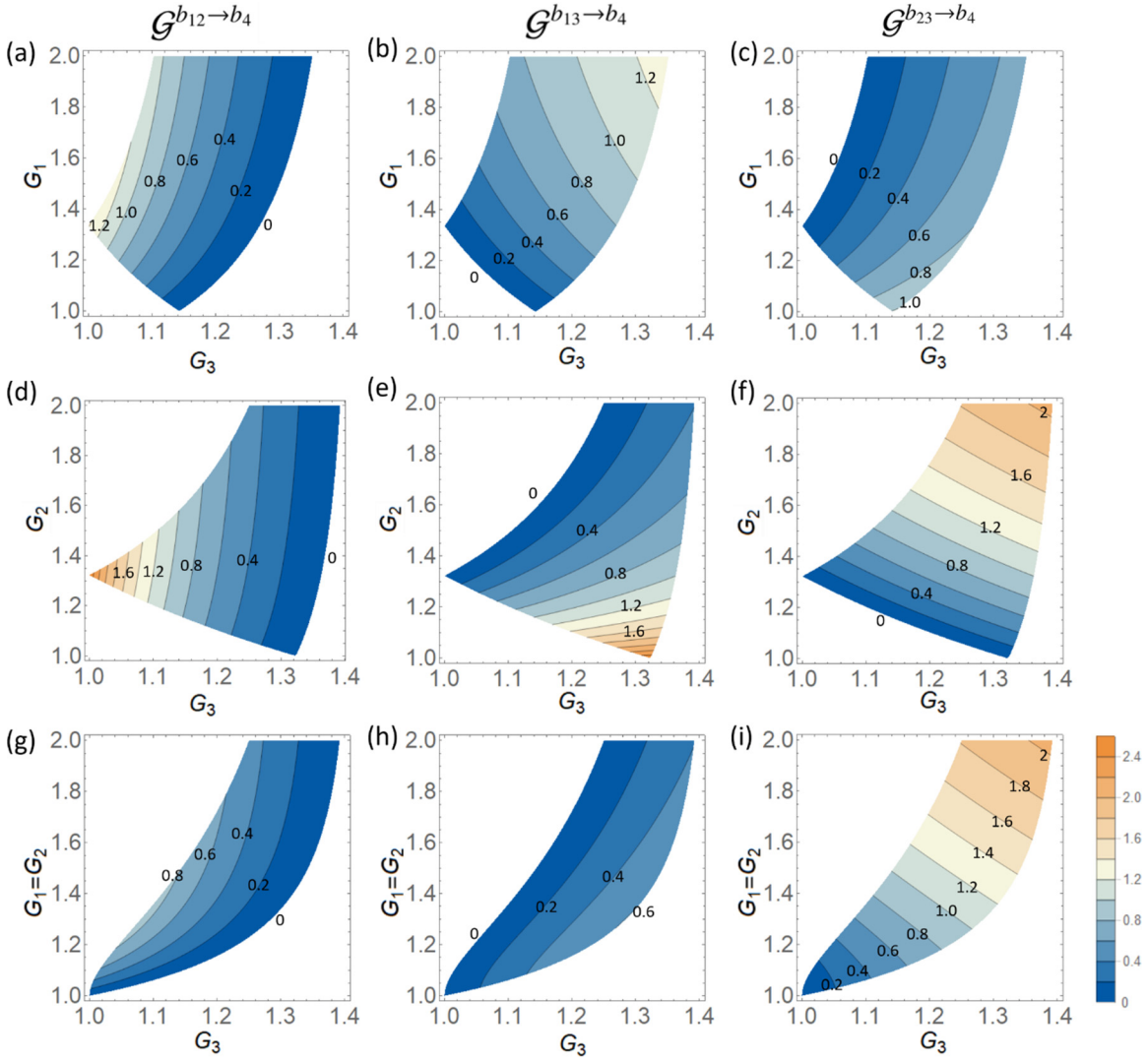

FIG. 7. Collective tripartite steering regions with the asymmetric structure of three cascaded FWMs, which are examined by the steerability of (2+1) mode > 0 and (1+1) mode $= 0$. The steering parameters $\mathcal{G}^{b_1b_2\to b_4}$, $\mathcal{G}^{b_1b_3\to b_4}$, and $\mathcal{G}^{b_2b_3\to b_4}$ as a function of (a)–(c) G_1 and G_3 for $G_2 = 1.2$, (d)–(f) G_2 and G_3 for $G_1 = 2$, and (g)–(i) $G_1 = G_2$ and G_3, respectively. In the white areas, the criteria of collective multipartite steering are not satisfied, and thus, the collective tripartite steering does not exist.

$(i = 0, 1, 2, 3)$ as the seed beam for the FWM_{i+1} process, as described in Fig. 8. The unitary transformation of the input-output relation corresponding to the five-mode state can be written as

$$\begin{bmatrix} \hat{X}_1^c \\ \hat{P}_1^c \\ \hat{X}_2^c \\ \hat{P}_2^c \\ \hat{X}_3^c \\ \hat{P}_3^c \\ \hat{X}_4^c \\ \hat{P}_4^c \\ \hat{X}_5^c \\ \hat{P}_5^c \end{bmatrix} = \begin{bmatrix} g_1 & 0 & G_1 & 0 & 0 & 0 & 0 & 0 & 0 & 0 \\ 0 & -g_1 & 0 & G_1 & 0 & 0 & 0 & 0 & 0 & 0 \\ G_1 g_2 & 0 & g_1 g_2 & 0 & G_2 & 0 & 0 & 0 & 0 & 0 \\ 0 & -G_1 g_2 & 0 & g_1 g_2 & 0 & G_2 & 0 & 0 & 0 & 0 \\ G_1 G_2 g_3 & 0 & g_1 G_2 g_3 & 0 & g_2 g_3 & 0 & G_3 & 0 & 0 & 0 \\ 0 & -G_1 G_2 g_3 & 0 & g_1 G_2 g_3 & 0 & g_2 g_3 & 0 & G_3 & 0 & 0 \\ G_1 G_2 G_3 g_4 & 0 & g_1 G_2 G_3 g_4 & 0 & g_2 G_3 g_4 & 0 & g_3 g_4 & 0 & G_4 & 0 \\ 0 & -G_1 G_2 G_3 g_4 & 0 & g_1 G_2 G_3 g_4 & 0 & g_2 G_3 g_4 & 0 & g_3 g_4 & 0 & G_4 \\ G_1 G_2 G_3 G_4 & 0 & g_1 G_2 G_3 G_4 & 0 & g_2 G_3 G_4 & 0 & g_3 G_4 & 0 & g_4 & 0 \\ 0 & G_1 G_2 G_3 G_4 & 0 & -g_1 G_2 G_3 G_4 & 0 & -g_2 G_3 G_4 & 0 & -g_3 G_4 & 0 & -g_4 \end{bmatrix} \begin{bmatrix} \hat{X}_{s_0} \\ \hat{P}_{s_0} \\ \hat{X}_{v_0} \\ \hat{P}_{v_0} \\ \hat{X}_{v_1} \\ \hat{P}_{v_1} \\ \hat{X}_{v_2} \\ \hat{P}_{v_2} \\ \hat{X}_{v_3} \\ \hat{X}_{v_3} \end{bmatrix}. \tag{9}$$

Collective quadripartite steering with the asymmetric-structure cascaded four-FWM system is shown in Fig. 9 while varying the (1+1)-, (2+1)-, and (3+1)-mode steering parameters with G_4 for fixed gain values of G_{1-3} (see the analytical solutions in the Appendix). In Fig. 9(a), modes $\hat{c}_1$, $\hat{c}_2$, $\hat{c}_3$, and $\hat{c}_4$ individually steer mode $\hat{c}_5$ for $G_1 = 1.2$ (line with circles) or 2 (line with squares), with $G_2 = G_3 = 1.2$. In Fig. 9(b), modes $\hat{c}_1$, $\hat{c}_2$, $\hat{c}_3$, and $\hat{c}_4$ individually steer mode $\hat{c}_5$ for $G_1 = G_3 = 1.2$, with $G_2 = 2$. According to the CKW monogamy relation in Eq. (3), we need to make sure that (2+1)-mode steerability is zero and (3+1)-mode steerability is larger than zero. For the $(\hat{c}_1, \hat{c}_2, \hat{c}_3) \to \hat{c}_5$ case, we quantify the (2+1)- and (3+1)-mode steering parameters with $G_1 = G_2 = G_3 = 1.2$. The steerabilities of modes $\hat{c}_1\hat{c}_2$, $\hat{c}_1\hat{c}_3$, $\hat{c}_2\hat{c}_3$, and $\hat{c}_1\hat{c}_2\hat{c}_3$ to mode $\hat{c}_5$ decrease when adjusting G_4 from 1 to 1.6 in Fig. 9(c). The steerabilities $\mathcal{G}^{c_1c_2\to c_5} = \mathcal{G}^{c_1c_3\to c_5} = \mathcal{G}^{c_2c_3\to c_5} = 0$, and $\mathcal{G}^{c_1c_2c_3\to c_5} > 0$ at $G_4 \in [1.171, 1.290)$, and the collective quadripartite steering is achieved. In the region of $G_4 \in [1.027, 1.114]$ $(G_1 = G_2 = G_3 = 1.2)$ in Fig. 9(d), mode $\hat{c}_5$ can be steered by $(\hat{c}_1, \hat{c}_2, \hat{c}_4)$ together but cannot be steered by any two modes $(\mathcal{G}^{c_1c_2c_4\to c_5} > 0$, $\mathcal{G}^{c_1c_2\to c_5} = \mathcal{G}^{c_1c_4\to c_5} = \mathcal{G}^{c_2c_4\to c_5} = 0)$. Similar phenomena are observed for the $(\hat{c}_2, \hat{c}_3, \hat{c}_4) \to \hat{c}_5$ case shown in Fig. 9(e), with fixed $G_1 = 2$, $G_2 = G_3 = 1.2$, $\mathcal{G}^{c_2c_3\to c_5} = \mathcal{G}^{c_2c_4\to c_5} = \mathcal{G}^{c_3c_4\to c_5} = 0$, and $\mathcal{G}^{c_2c_3c_4\to c_5} > 0$ at $G_4 \in [1.075, 1.126]$. It is also seen that with fixed $G_1 = G_3 = 1.2$ and $G_2 = 2$, the steerabilities $\mathcal{G}^{c_1c_3\to c_5} = \mathcal{G}^{c_1c_4\to c_5} = \mathcal{G}^{c_3c_4\to c_5} = 0$ at $G_4 \in (1.078, 1.126]$, but $\mathcal{G}^{c_1c_3c_4\to c_5} > 0$, as shown in Fig. 9(f). Interestingly, our system has a very unique property of entanglement distribution; that is, the group of all the idler (signal) beams can always steer the signal (idler) one. Hence, it is helpful for achieving large-scale collective multipartite steering while signal and idler beam numbers are unequal. The results show that the collective multipartite steering can be extended with more parties by asymmetric cascaded Rb vapors. Also, the unequal number of the output modes via the asymmetric structure and the corresponding quantum property suggest the asymmetric nature of the quantum correlation distribution within the collective steering defined in Eq. (2). Moreover, by introducing optical loss, collective pentapartite steering in the asymmetric structure can be created, as detailed in Sec. IV.

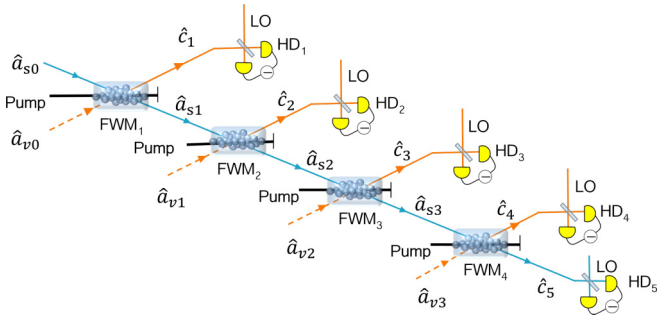

FIG. 8. Schematic diagram of the production of the five-mode entangled state via an asymmetric structure. $\hat{a}_{si}(i = 0, 1, 2, 3)$ is seeded into FWM_1, FWM_2, FWM_3, and FWM_4. $\hat{a}_{vi}$ $(i = 0, 1, 2, 3)$ are the vacuum input modes; $\hat{c}_{1-5}$ are the final output modes. LO denotes the local oscillator for homodyne detection (HD_{1-5}).

IV. EFFECT OF OPTICAL LOSS ON COLLECTIVE MULTIPARTITE STEERING

Taking into account imperfect optical devices, optical propagation, and detection efficiency, optical loss is unavoidable in practical situations. Therefore, it is necessary to investigate the loss effect on the collective steering in two structures. For simplicity, we place a beam splitter in front of the photodetector to introduce some vacuum noise. Then all of the output modes can be modified as $\hat{a}'_{1-4} = \sqrt{\eta}_{1-4}\hat{a}_{1-4} - \sqrt{1-\eta_{1-4}}\hat{v}_{1-4}$, where η_{1-4} is the transmissivity of the beam splitters in different channels and $1 - \eta_{1-4}$ is the optical loss [58,59]. Similarly, we define the output modes $\hat{b}'_{1-4}$ and $\hat{c}'_{1-5}$ in the asymmetric structures.

In the symmetric four-mode scenario, we fix parametric gains $G_1 = G_2 = G_3 = 1.2$ and set $\eta_1 = \eta_2 = \eta_3 = \eta$, $\eta_4 = 0.9$, and the steerabilities $\mathcal{G}^{a'_1a'_2a'_3\to a'_4}$ and $\mathcal{G}^{a'_1a'_3\to a'_4}$ always equal zero with $\eta = 0.5$ at the same time, as indicated in Fig. 10(a). We increase the gain to 2 in Fig. 10(b) and get the same result. So collective quadripartite steering cannot be achieved by adjusting gain and loss in the symmetric case. Then, we investigate the collective steerability in the asymmetric four-mode scenario with the same G and η.

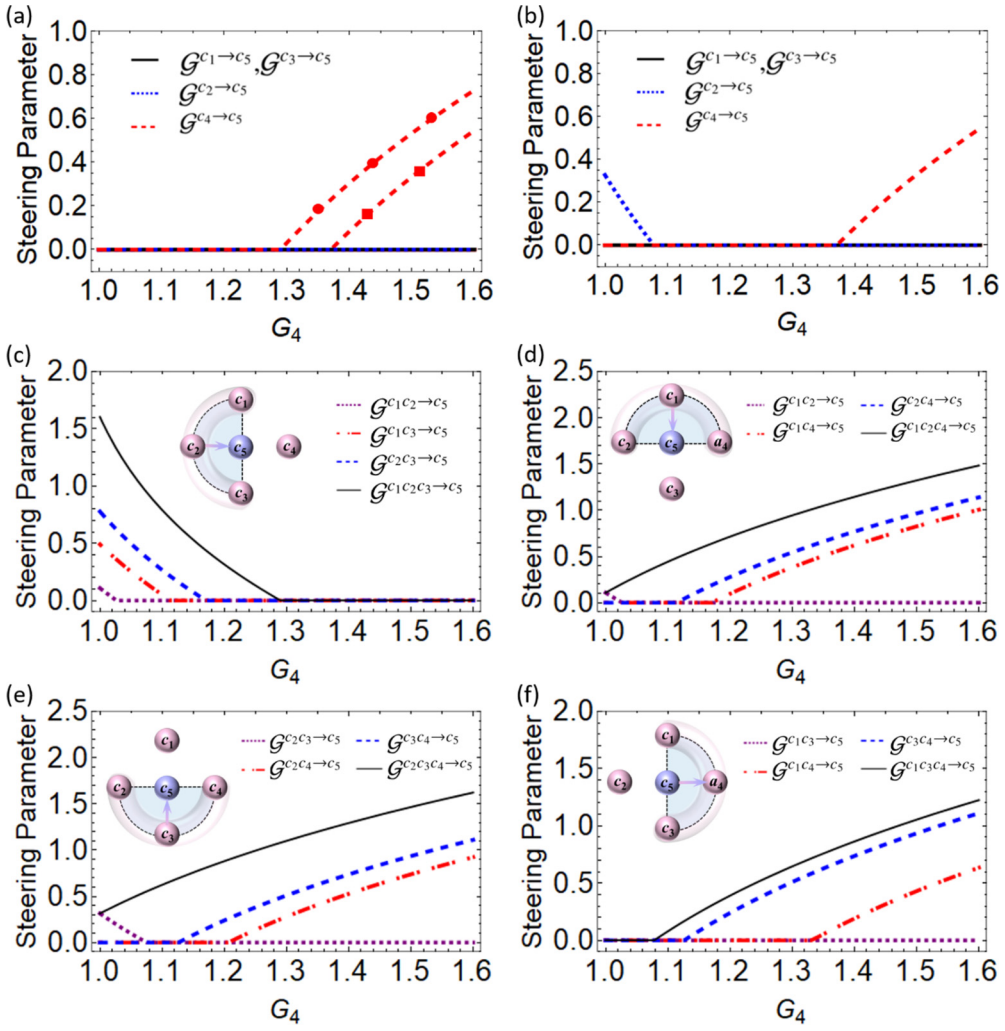

FIG. 9. Collective quadripartite steering with an asymmetric-structure cascaded four-FWM system. Variation of the (1+1)-, (2+1)-, and (3+1)-mode steering parameters with G_4 for fixed gain values of G_{1-3}. $\hat{c}_1$, $\hat{c}_2$, $\hat{c}_3$, and $\hat{c}_4$ are the idler beams; $\hat{c}_5$ is the signal beam. (a) Modes $\hat{c}_1$, $\hat{c}_2$, $\hat{c}_3$, and $\hat{c}_4$ individually steer mode $\hat{c}_5$ for $G_1 = 1.2$ (line with circles) or 2 (line with squares), $G_2 = G_3 = 1.2$. (b) Modes $\hat{c}_1$, $\hat{c}_2$, $\hat{c}_3$, and $\hat{c}_4$ individually steer mode $\hat{c}_5$ for $G_1 = G_3 = 1.2$, $G_2 = 2$. (c) Modes $\hat{c}_1\hat{c}_2$, $\hat{c}_1\hat{c}_3$, $\hat{c}_2\hat{c}_3$, and $\hat{c}_1\hat{c}_2\hat{c}_3$ steer mode $\hat{c}_5$ for $G_1 = G_2 = G_3 = 1.2$. (d) Modes $\hat{c}_1\hat{c}_2$, $\hat{c}_1\hat{c}_4$, $\hat{c}_2\hat{c}_4$, and $\hat{c}_1\hat{c}_2\hat{c}_4$ steer mode $\hat{c}_5$ for $G_1 = G_2 = G_3 = 1.2$. (e) Modes $\hat{c}_2\hat{c}_3$, $\hat{c}_2\hat{c}_4$, $\hat{c}_3\hat{c}_4$, and $\hat{c}_2\hat{c}_3\hat{c}_4$ steer mode $\hat{c}_5$ for $G_1 = 2$, $G_2 = G_3 = 1.2$. (f) Modes $\hat{c}_1\hat{c}_3$, $\hat{c}_1\hat{c}_4$, $\hat{c}_3\hat{c}_4$, and $\hat{c}_1\hat{c}_3\hat{c}_4$ steer mode $\hat{c}_5$ for $G_1 = G_3 = 1.2$, $G_2 = 2$.

In the asymmetric-structure case, the collective steerability can be obtained remarkably, as shown in Figs. 10(c) and 10(d). The largest steerability $\mathcal{G}^{b_1'b_2'b_3'\to b_4'}$ is 0.338, with $\eta = 0.642$, and $\mathcal{G}^{b_1'b_2'\to b_4'} = \mathcal{G}^{b_2'b_3'\to b_4'} = \mathcal{G}^{b_1'b_3'\to b_4'} = 0$ in Fig. 10(c). Hence, the amount of steerability is larger than $\ln(e/2)$ and meets the condition of 1SDI QSS with nonzero key rates [20]. The dealer $\hat{b}_4'$ sends a secret, and receivers ($\hat{b}_1'$, $\hat{b}_2'$, and $\hat{b}_3'$) can decode the information only by collaborating; any one of the receivers is indispensable. When the gain parameters $G_1 = G_2 = G_3$ increase to 2, the steerabilities $\mathcal{G}^{b_2'b_3'\to b_4'}$ and $\mathcal{G}^{b_1'b_3'\to b_4'}$ also increase and become more sensitive to the loss. Therefore, for the collective steering $[(b_1', b_2', b_3') \to b_4']$, it is possible, by introducing more losses, to make $\mathcal{G}^{b_2'b_3'\to b_4'}$ and $\mathcal{G}^{b_1'b_3'\to b_4'}$ equal zero while $\mathcal{G}^{b_1'b_2'b_3'\to b_4'}$ is larger than zero. The largest steerability $\mathcal{G}^{b_1'b_2'b_3'\to b_4'}$ is decreased to 0.088 at $\eta = 0.525$, and the collective-steering region changes in Fig. 10(d). After the calculation of two four-mode systems, we extend this protocol to an asymmetric five-mode case. Figure 10(e) shows that the collective pentapartite steering can be obtained based on four cascaded FWMs and by adjusting the transmissivity η. The maximum steerability $\mathcal{G}^{c_1'c_2'c_3'c_4'\to b_5'}$ is 0.264 with $\eta_1 = \eta_2 = \eta_3 = \eta_4 = \eta = 0.577$, $\eta_5 = 0.9$, and $\mathcal{G}^{c_1'c_2'c_3'\to b_5'} = \mathcal{G}^{c_1'c_2'c_4'\to b_5'} = \mathcal{G}^{c_1'c_3'c_4'\to b_5'} = \mathcal{G}^{c_2'c_3'c_4'\to b_5'} = 0$. When the parametric gain $G_1 = G_2 = G_3 = G_4$ is increased to 1.5, the maximum steerability $\mathcal{G}^{c_1'c_2'c_3'c_4'\to b_5'}$ is decreased to 0.092, and the collective-steering region is reduced to $\eta \in (0.5, 0.527]$, as shown in Fig. 10(f). Because of the difference in internal entanglement distributions in the two schemes, the sensitivity of collective steering to loss is different. Cascading more Rb vapors in the asymmetric structure can build higher-party collective steering in the system.

In general, the loss needs to be overcome because it will weaken the quantum correlation among different modes. Interestingly, we find that loss has a positive effect on achieving the collective steering. And larger parametric gain is not always better. Here, by jointly adjusting the parametric gain and the transmissivity of the beam splitter, the collective-

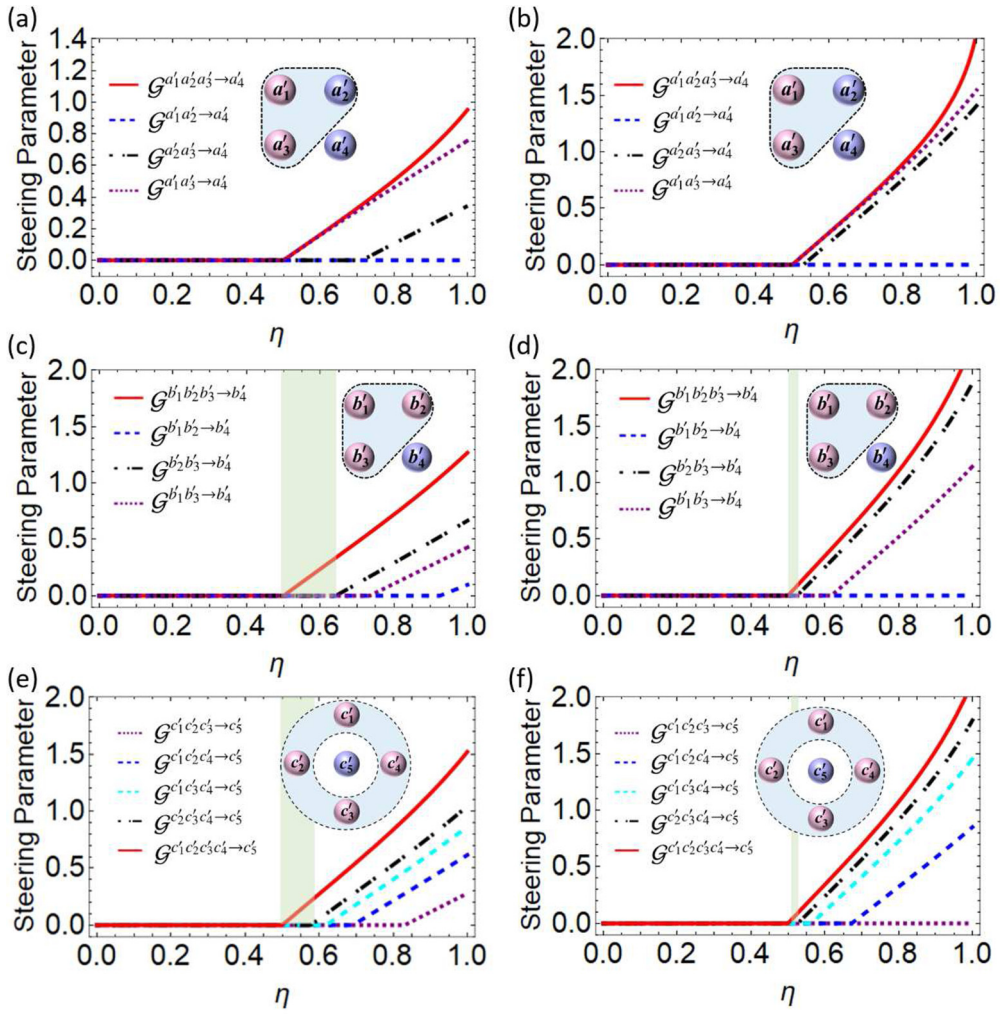

FIG. 10. Loss effect on collective steering for two structures with different FWM gains. (a) and (b) The symmetric four-mode system with $\eta_1 = \eta_2 = \eta_3 = \eta$, $\eta_4 = 0.9$, $G_1 = G_2 = G_3 = 1.2$ and 2, respectively. (c) and (d) The asymmetric four-mode system with $\eta_1 = \eta_2 = \eta_3 = \eta$, $\eta_4 = 0.9$, $G_1 = G_2 = G_3 = 1.2$ and 2, respectively. (e) and (f) The asymmetric five-mode system with $\eta_1 = \eta_2 = \eta_3 = \eta_4 = \eta$, $\eta_5 = 0.9$, $G_1 = G_2 = G_3 = G_4 = 1.2$ and 1.5, respectively. The light green shaded areas represent the collective-steering region.

steering region can be obtained with more parties. Therefore, nontrivially, introducing optical loss might be useful for implementing QSS tasks in practice.

V. SUMMARY

In summary, we have theoretically studied the collective multipartite EPR steering properties of multimode Gaussian entangled states. Those states can be produced by cascading FWM processes in Rb atomic vapors symmetrically and asymmetrically. According to the CKW monogamy relations for Gaussian steering, we simplified the collective-steering criterion. We investigated the steering properties shared among four- and five-mode states, which could be actively modulated by changing the parametric gain values of FWM in both structures. With the analytical solutions of the steering parameter upon the gain values, for pure four-mode states, we obtained six partitions of collective tripartite steering in the symmetric structure and three partitions in the asymmetric one for pure four-mode states. Interestingly, although versatile collective steering can be obtained, we found that there is no collective quadripartite EPR steering when the four-mode states in both structures are pure. Furthermore, our scheme can be extended to construct collective quadripartite steering [e.g., $(\hat{c}_1, \hat{c}_2, \hat{c}_3) \to \hat{c}_5$, $(\hat{c}_1, \hat{c}_2, \hat{c}_4) \to \hat{c}_5$, $(\hat{c}_2, \hat{c}_3, \hat{c}_4) \to \hat{c}_5$, and $(\hat{c}_1, \hat{c}_3, \hat{c}_4) \to \hat{c}_5$)] in asymmetric five-mode entangled states by cascading more FWMs. Finally, we found that introducing the optical loss can assist in creating collective multipartite steering only in the asymmetric structure. By introducing optical loss in the steering modes, the collective quadripartite $[(\hat{b}'_1, \hat{b}'_2, \hat{b}'_3) \to \hat{b}'_4]$ and pentapartite $[(\hat{c}'_1, \hat{c}'_2, \hat{c}'_3, \hat{c}'_4) \to \hat{c}'_5]$ steerings were produced in the asymmetric structure. Our results indicate that the cascaded FWM processes can provide a promising and scalable platform for the 1SDI-QSS.

Moreover, our method is general for treating all large-scale Gaussian states via multimode parametric amplification processes [60,61]. The cascaded four-wave mixing scheme in combination with a mode-dependent non-Gaussian operation, such as photon subtraction on a specific mode, is useful for remotely generating a Wigner-negative entangled state in CV multimode cluster states [62–64].

ACKNOWLEDGMENTS

The authors gratefully acknowledge Q. He and Y. Xiang for helpful discussions. The authors recognize the National Key R&D Program of China (Grant No. 2017YFA0303700), the National Natural Science Foundation of China (Grants No. 11904279, No. 61975159, No. 12074303, and No. 12174302), the National Science Foundation of Jiangsu Province (Grant No. BK20180322), and the Key Scientific and Technological Innovation Team of Shaanxi Province (Grant No. 2021TD-56). Y.L. also thanks the China Scholarship Council for financial support.

APPENDIX

1. CM of a four-mode state of the symmetric structure for $G_1 = 2$ and $G_2 = G_3 = 1.2$

$$\sigma_{\mathrm{sym4}} = \begin{pmatrix} 10.520 & 0 & 6.3679 & 0 & 5.5148 & 0 & 9.9766 & 0 \\ 0 & 10.520 & 0 & -6.3679 & 0 & 5.5148 & 0 & -9.9766 \\ 6.3679 & 0 & 4.5200 & 0 & 3.0484 & 0 & 5.5148 & 0 \\ 0 & -6.3679 & 0 & 4.5200 & 0 & -3.0484 & 0 & 5.5148 \\ 5.5148 & 0 & 3.0484 & 0 & 4.5200 & 0 & 6.3679 & 0 \\ 0 & 5.5148 & 0 & -3.0484 & 0 & 4.5200 & 0 & -6.3679 \\ 9.9766 & 0 & 5.5148 & 0 & 6.3679 & 0 & 10.520 & 0 \\ 0 & -9.9766 & 0 & 5.5148 & 0 & -6.3679 & 0 & 10.520 \end{pmatrix}. \tag{A1}$$

2. CM of a four-mode state of the asymmetric structure for $G_1 = 2$ and $G_2 = G_3 = 1.2$

$$\sigma_{\mathrm{asy4}} = \begin{pmatrix} 7.0000 & 0 & 4.5957 & 0 & 5.5148 & 0 & 9.9766 & 0 \\ 0 & 7.0000 & 0 & 4.5957 & 0 & 5.5148 & 0 & -9.9766 \\ 4.5957 & 0 & 4.5200 & 0 & 4.2240 & 0 & 7.6415 & 0 \\ 0 & 4.5957 & 0 & 4.5200 & 0 & 4.2240 & 0 & -7.6415 \\ 5.5148 & 0 & 4.2240 & 0 & 6.0688 & 0 & 9.1698 & 0 \\ 0 & 5.5148 & 0 & 4.2240 & 0 & 6.0688 & 0 & -9.1698 \\ 9.9766 & 0 & 7.6415 & 0 & 9.1698 & 0 & 15.589 & 0 \\ 0 & -9.9766 & 0 & -7.6415 & 0 & -9.1698 & 0 & 15.589 \end{pmatrix}. \tag{A2}$$

3. CM of a five-mode state of the asymmetric structure for $G_1 = 2$, $G_2 = G_3 = 1.2$, and $G_4 = 1.1$

$$\sigma_{asy5} = \begin{pmatrix} 7.0000 & 0 & 4.5957 & 0 & 5.5148 & 0 & 4.5719 & 0 & 10.974 & 0 \\ 0 & 7.0000 & 0 & 4.5957 & 0 & 5.5148 & 0 & 4.5719 & 0 & -10.974 \\ 4.5957 & 0 & 4.5200 & 0 & 4.2240 & 0 & 3.5018 & 0 & 8.4057 & 0 \\ 0 & 4.5957 & 0 & 4.5200 & 0 & 4.2240 & 0 & 3.5018 & 0 & -8.4057 \\ 5.5148 & 0 & 4.2240 & 0 & 6.0688 & 0 & 4.2021 & 0 & 10.087 & 0 \\ 0 & 5.5148 & 0 & 4.2240 & 0 & 6.0688 & 0 & 4.2021 & 0 & -10.087 \\ 4.5719 & 0 & 3.5018 & 0 & 4.2021 & 0 & 4.4836 & 0 & 8.3621 & 0 \\ 0 & 4.5719 & 0 & 3.5018 & 0 & 4.2021 & 0 & 4.4836 & 0 & -8.3621 \\ 10.974 & 0 & 8.4057 & 0 & 10.087 & 0 & 8.3621 & 0 & 19.072 & 0 \\ 0 & -10.974 & 0 & -8.4057 & 0 & -10.087 & 0 & -8.3621 & 0 & 19.072 \end{pmatrix}. \tag{A3}$$

4. Solution to (1+1)-, (2+1)-, (3+1)-, and (4+1)-mode EPR steering in a five-mode state of the asymmetric structure, $G_1 > 1$, $G_2 > 1$, $G_3 > 1$, and $G_4 > 1$

$$\mathcal{G}^{c_1\to c_5} = \max\left\{0, -\ln\left(\frac{2G_1^2G_2^2G_3^2G_4^2 - 2G_1^2 + 1}{2G_1^2 - 1}\right)\right\}, \tag{A4a}$$

$$\mathcal{G}^{c_2\to c_5} = \max\left\{0, -\ln\left(\frac{2G_1^2G_2^2G_3^2G_4^2 - 2G_1^2G_2^2 + 2G_1^2 - 1}{2G_1^2G_2^2 - 2G_1^2 + 1}\right)\right\}, \tag{A4b}$$

$$\mathcal{G}^{c_3\to c_5} = \max\left\{0, -\ln\left(\frac{2G_1^2G_2^2G_3^2G_4^2 - 2G_1^2G_2^2G_3^2 + 2G_1^2G_2^2 - 1}{2G_1^2G_2^2G_3^2 - 2G_1^2G_2^2 + 1}\right)\right\}, \tag{A4c}$$

$$\mathcal{G}^{c_4\to c_5} = \max\left\{0, -\ln\left(\frac{2G_1^2G_2^2G_3^2 - 1}{2G_1^2G_2^2G_3^2G_4^2 - 2G_1^2G_2^2G_3^2 + 1}\right)\right\}, \tag{A4d}$$

$$\mathcal{G}^{c_1c_2\to c_5} = \max\left\{0, -\ln\left(\frac{2G_1^2G_2^2G_3^2G_4^2 - 2G_1^2G_2^2 + 1}{2G_1^2G_2^2 - 1}\right)\right\}, \tag{A4e}$$

$$\mathcal{G}^{c_1c_3\to c_5} = \max\left\{0, -\ln\left(\frac{2G_1^2G_2^2G_3^2G_4^2 - 2G_1^2G_2^2G_3^2 + 2G_1^2G_2^2 - 2G_1^2 + 1}{2G_1^2G_2^2G_3^2 - 2G_1^2G_2^2 + 2G_1^2 - 1}\right)\right\}, \tag{A4f}$$

$$\mathcal{G}^{c_1c_4\to c_5} = \max\left\{0, -\ln\left(\frac{2G_1^2G_2^2G_3^2 - 2G_1^2 + 1}{2G_1^2G_2^2G_3^2G_4^2 - 2G_1^2G_2^2G_3^2 + 2G_1^2 - 1}\right)\right\}, \tag{A4g}$$

$$\mathcal{G}^{c_2c_3\to c_5} = \max\left\{0, -\ln\left(\frac{2G_1^2G_2^2G_3^2G_4^2 - 2G_1^2G_2^2G_3^2 + 2G_1^2 - 1}{2G_1^2G_2^2G_3^2 - 2G_1^2 + 1}\right)\right\}, \tag{A4h}$$

$$\mathcal{G}^{c_2c_4\to c_5} = \max\left\{0, -\ln\left(\frac{2G_1^2G_2^2G_3^2 - 2G_1^2G_2^2 + 2G_1^2 - 1}{2G_1^2G_2^2G_3^2G_4^2 - 2G_1^2G_2^2G_3^2 + 2G_1^2G_2^2 - 2G_1^2 + 1}\right)\right\}, \tag{A4i}$$

$$\mathcal{G}^{c_3c_4\to c_5} = \max\left\{0, -\ln\left(\frac{2G_1^2G_2^2 - 1}{2G_1^2G_2^2G_3^2G_4^2 - 2G_1^2G_2^2 + 1}\right)\right\}, \tag{A4j}$$

$$\mathcal{G}^{c_1c_2c_3\to c_5} = \max\left\{0, -\ln\left(\frac{2G_1^2G_2^2G_3^2G_4^2 - 2G_1^2G_2^2G_3^2 + 1}{2G_1^2G_2^2G_3^2 - 1}\right)\right\}, \tag{A4k}$$

$$\mathcal{G}^{c_1c_2c_4\to c_5} = \max\left\{0, -\ln\left(\frac{2G_1^2G_2^2G_3^2 - 2G_1^2G_2^2 + 1}{2G_1^2G_2^2G_3^2G_4^2 - 2G_1^2G_2^2G_3^2 + 2G_1^2G_2^2 - 1}\right)\right\}, \tag{A4l}$$

$$\mathcal{G}^{c_1c_3c_4\to c_5} = \max\left\{0, -\ln\left(\frac{2G_1^2G_2^2 - 2G_1^2 + 1}{2G_1^2G_2^2G_3^2G_4^2 - 2G_1^2G_2^2 + 2G_1^2 - 1}\right)\right\}, \tag{A4m}$$

$$\mathcal{G}^{c_2c_3c_4\to c_5} = \max\left\{0, -\ln\left(\frac{2G_1^2 - 1}{2G_1^2G_2^2G_3^2G_4^2 - 2G_1^2 + 1}\right)\right\}, \tag{A4n}$$

$$\mathcal{G}^{c_1c_2c_3c_4\to c_5} = \max\left\{0, -\ln\left(\frac{1}{2G_1^2G_2^2G_3^2G_4^2 - 1}\right)\right\}. \tag{A4o}$$

[1] A. Einstein, B. Podolsky, and N. Rosen, Phys. Rev. **47**, 777 (1935).
[2] M. D. Reid, Phys. Rev. A **40**, 913 (1989).
[3] H. M. Wiseman, S. J. Jones, and A. C. Doherty, Phys. Rev. Lett. **98**, 140402 (2007).
[4] S. J. Jones, H. M. Wiseman, and A. C. Doherty, Phys. Rev. A **76**, 052116 (2007).
[5] M. D. Reid, P. D. Drummond, W. P. Bowen, E. G. Cavalcanti, P. K. Lam, H. A. Bachor, U. L. Andersen, and G. Leuchs, Rev. Mod. Phys. **81**, 1727 (2009).
[6] C. Branciard, E. G. Cavalcanti, S. P. Walborn, V. Scarani, and H. M. Wiseman, Phys. Rev. A **85**, 010301(R) (2012).
[7] N. Walk, S. Hosseini, J. Geng, O. Thearle, J. Y. Haw, S. Armstrong, S. M. Assad, J. Janousek, T. C. Ralph, T. Symul, H. M. Wiseman, and P. K. Lam, Optica **3**, 634 (2016).
[8] M. D. Reid, Phys. Rev. A **88**, 062338 (2013).
[9] Q. Y. He, L. Rosales-Zárate, G. Adesso, and M. D. Reid, Phys. Rev. Lett. **115**, 180502 (2015).
[10] C.-Y. Chiu, N. Lambert, T.-L. Liao, F. Nori, and C.-M. Li, npj Quantum Inf. **2**, 16020 (2016).
[11] R. Uola, A. C. S. Costa, H. C. Nguyen, and O. Gühne, Rev. Mod. Phys. **92**, 015001 (2020).
[12] M. Piani and J. Watrous, Phys. Rev. Lett. **114**, 060404 (2015).
[13] T. Moroder, O. Gittsovich, M. Huber, and O. Gühne, Phys. Rev. Lett. **113**, 050404 (2014).
[14] S. Yu and C. H. Oh, Phys. Rev. A **95**, 032111 (2017).
[15] Q. Y. He and M. D. Reid, Phys. Rev. Lett. **111**, 250403 (2013).
[16] S. Armstrong, W. Meng, R. Y. Teh, Q. Gong, Q. He, J. Janousek, H. A. Bachor, M. D. Reid, and K. L. Ping, Nat. Phys. **11**, 167 (2015).
[17] X. Deng, Y. Xiang, C. Tian, G. Adesso, Q. He, Q. Gong, X. Su, C. Xie, and K. Peng, Phys. Rev. Lett. **118**, 230501 (2017).
[18] Y. Cai, Y. Xiang, Y. Liu, Q. He, and N. Treps, Phys. Rev. Res. **2**, 032046(R) (2020).
[19] M. Wang, Y. Xiang, H. Kang, D. Han, Y. Liu, Q. He, Q. Gong, X. Su, and K. Peng, Phys. Rev. Lett. **125**, 260506 (2020).
[20] Y. Xiang, I. Kogias, G. Adesso, and Q. He, Phys. Rev. A **95**, 010101(R) (2017).
[21] I. Kogias, Y. Xiang, Q. He, and G. Adesso, Phys. Rev. A **95**, 012315 (2017).
[22] Y. Xiang, F. Sun, Q. He, and Q. Gong, Fundam. Res. **1**, 99 (2021).
[23] R. Cleve, D. Gottesman, and H.-K. Lo, Phys. Rev. Lett. **83**, 648 (1999).
[24] A. Karlsson, M. Koashi, and N. Imoto, Phys. Rev. A **59**, 162 (1999).
[25] D. Gottesman, Phys. Rev. A **61**, 042311 (2000).
[26] M. Hillery, V. Bužek, and A. Berthiaume, Phys. Rev. A **59**, 1829 (1999).
[27] D. Markham and B. C. Sanders, Phys. Rev. A **78**, 042309 (2008).

[28] Y. Zhou, J. Yu, Z. Yan, X. Jia, J. Zhang, C. Xie, and K. Peng, Phys. Rev. Lett. **121**, 150502 (2018).
[29] M. Wang, Q. Gong, and Q. He, Opt. Lett. **39**, 6703 (2014).
[30] C. F. McCormick, V. Boyer, E. Arimondo, and P. D. Lett, Opt. Lett. **32**, 178 (2007).
[31] Y. Cai, J. Feng, H. Wang, G. Ferrini, X. Xu, J. Jing, and N. Treps, Phys. Rev. A **91**, 013843 (2015).
[32] A. M. Marino, R. C. Pooser, V. Boyer, and P. D. Lett, Nature (London) **457**, 859 (2009).
[33] R. C. Pooser, A. M. Marino, V. Boyer, K. M. Jones, and P. D. Lett, Phys. Rev. Lett. **103**, 010501 (2009).
[34] B. J. Lawrie, P. G. Evans, and R. C. Pooser, Phys. Rev. Lett. **110**, 156802 (2013).
[35] Z. Qin, L. Cao, H. Wang, A. M. Marino, W. Zhang, and J. Jing, Phys. Rev. Lett. **113**, 023602 (2014).
[36] F. Hudelist, J. Kong, C. Liu, J. Jing, Z. Y. Ou, and W. Zhang, Nat. Commun. **5**, 3049 (2014).
[37] V. Boyer, A. M. Marino, R. C. Pooser, and P. D. Lett, Science **321**, 544 (2008).
[38] R. M. Camacho, P. K. Vudyasetu, and J. C. Howell, Nat. Photonics **3**, 103 (2009).
[39] J. B. Clark, R. T. Glasser, Q. Glorieux, U. Vogl, T. Li, K. M. Jones, and P. D. Lett, Nat. Photonics **8**, 515 (2014).
[40] H. Wang, A. M. Marino, and J. Jing, Appl. Phys. Lett. **107**, 121106 (2015).
[41] J. Liu, W. Liu, S. Li, D. Wei, H. Gao, and F. Li, Photonics Res. **5**, 617 (2017).
[42] N. V. Corzo, A. M. Marino, K. M. Jones, and P. D. Lett, Phys. Rev. Lett. **109**, 043602 (2012).
[43] C. S. Embrey, M. T. Turnbull, P. G. Petrov, and V. Boyer, Phys. Rev. X **5**, 031004 (2015).
[44] D. Zhang, C. Li, Z. Zhang, Y. Zhang, Y. Zhang, and M. Xiao, Phys. Rev. A **96**, 043847 (2017).
[45] X. Pan, S. Yu, Y. Zhou, K. Zhang, K. Zhang, S. Lv, S. Li, W. Wang, and J. Jing, Phys. Rev. Lett. **123**, 070506 (2019).
[46] S. Li, X. Pan, Y. Ren, H. Liu, S. Yu, and J. Jing, Phys. Rev. Lett. **124**, 083605 (2020).
[47] K. Zheng, M. Mi, B. Wang, L. Xu, L. Hu, S. Liu, Y. Lou, J. Jing, and L. Zhang, Photonics Res. **8**, 1653 (2020).
[48] L. Wang, S. Lv, and J. Jing, Opt. Express **25**, 17457 (2017).
[49] Y. Liu, Y. Cai, Y. Xiang, F. Li, Y. Zhang, and Q. He, Opt. Express **27**, 33070 (2019).
[50] Y. Xiang, Y. Liu, Y. Cai, F. Li, Y. Zhang, and Q. He, Phys. Rev. A **101**, 053834 (2020).
[51] I. Kogias, A. R. Lee, S. Ragy, and G. Adesso, Phys. Rev. Lett. **114**, 060403 (2015).
[52] L. Lami, C. Hirche, G. Adesso, and A. Winter, Phys. Rev. Lett. **117**, 220502 (2016).
[53] M. D. Reid, Phys. Rev. A **88**, 062108 (2013).
[54] M. Wang, Y. Xiang, Q. He, and Q. Gong, Phys. Rev. A **91**, 012112 (2015).
[55] C. F. McCormick, A. M. Marino, V. Boyer, and P. D. Lett, Phys. Rev. A **78**, 043816 (2008).
[56] S.-W. Ji, M. S. Kim, and H. Nha, J. Phys. A **48**, 135301 (2015).
[57] G. Adesso and R. Simon, J. Phys. A **49**, 34LT02 (2016).
[58] B. Yurke and D. Stoler, Phys. Rev. Lett. **57**, 13 (1986).
[59] H. P. Yuen and V. W. S. Chan, Opt. Lett. **8**, 177 (1983).
[60] K. Zhang, W. Wang, S. Liu, X. Pan, J. Du, Y. Lou, S. Yu, S. Lv, N. Treps, C. Fabre, and J. Jing, Phys. Rev. Lett. **124**, 090501 (2020).
[61] Y. Cai, L. Hao, D. Zhang, Y. Liu, B. Luo, Z. Zheng, F. Li, and Y. Zhang, Opt. Express **28**, 25278 (2020).
[62] Y.-S. Ra, A. Dufour, M. Walschaers, C. Jacquard, T. Michel, C. Fabre, and N. Treps, Nat. Phys. **16**, 144 (2020).
[63] M. Walschaers and N. Treps, Phys. Rev. Lett. **124**, 150501 (2020).
[64] M. Zhang, H. Kang, M. Wang, F. Xu, X. Su, and K. Peng, Photonics Res. **9**, 887 (2021).